Geochemistry Geophysics Geosystems G3
AN ELECTRONIC JOURNAL OF THE EARTH SCIENCES
Published by AGU and the Geochemical Society

Article
Volume 6, Number 8
5 August 2005
Q08002, doi:10.1029/2004GC000818
ISSN: 1525-2027

Vug waves: A mechanism for coupled rock deformation and fluid migration

Jason Phipps Morgan
Department of Geological Sciences, Cornell University, 4164 Snee Hall, Ithaca, New York 14853, USA (jp369@cornell.edu)

Benjamin K. Holtzman
Department of Geology and Geophysics, University of Minnesota, Minneapolis, Minnesota 55455, USA (holtz007@tc.umn.edu)

[1] Vug waves are a joint deformation/fluid-migration mechanism in which a rock deforms by the movement of a penny-shaped, fluid-filled crack dislocation across a plane of shear, with migration of the crack and fluid driven by the release of elastic shear strain energy. Vug waves (here so named because a "vug" is a hole in the Earth and "wave" implies that it moves) may provide an effective means for (1) rapidly migrating and focusing relatively isolated batches of melt to mid-ocean ridge axes, (2) a possible origin for weakness and rheological and seismic anisotropy of Earth's asthenosphere, and (3) the origin of large, weak shear zones within Earth's mantle and crust. The existence of vug waves would also imply that in many geologic environments the strain-energy release from migrating a fluid-filled crack through a stressed solid may play a larger role in shaping fluid migration than the buoyancy of the fluid with respect to its host rock.

Components: 9915 words, 7 figures, 1 table.

Keywords: melt migration; rock deformation.

Index Terms: 3902 Mineral Physics: Creep and deformation; 8159 Tectonophysics: Rheology: crust and lithosphere (8031); 8434 Volcanology: Magma migration and fragmentation.

Received 18 August 2004; **Revised** 8 March 2005; **Accepted** 25 March 2005; **Published** 5 August 2005.

Phipps Morgan, J., and B. K. Holtzman (2005), Vug waves: A mechanism for coupled rock deformation and fluid migration, *Geochem. Geophys. Geosyst.*, *6*, Q08002, doi:10.1029/2004GC000818.

1. Introduction

[2] In spite of the fundamental importance of magma transport in creating and feeding volcanic activity, the mechanisms of deep melt transport remain obscure. In the progression from mantle to surface, the matrix deforms initially as a highly viscous fluid at depth; as melt rises toward the cooler surface, the elastic properties of the matrix increasingly dominate the melt migration process. Thus every parcel of melt that reaches the surface is likely to travel through the mantle and crust by a range of mechanisms, as sketched in Figure 1. Theoretical and observational studies have primarily focused on two potential mechanisms of melt migration, porous flow and tensile dike propagation (Figure 1), both driven by buoyancy of the melt, and a closely related mechanism in which melt segregation occurs by a reaction-infiltration instability. (These mechanisms will be further described in the next paragraph.) Another class of mechanisms, much less studied, involves melt migration, segregation, and self-organization driven by the differential stresses due to convection and/or plate spreading that are also driving the deformation of the solid. Examples of these mechanisms have been studied in experiments, at conditions where the matrix deforms predominantly by ductile creep

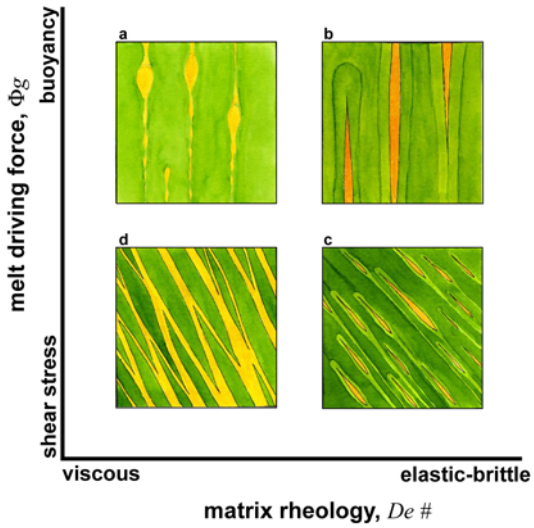

Figure 1. Melt migration mechanism map. This 2-D space defines regimes of melt migration mechanisms defined by matrix behavior and driving force for melt migration. The horizontal axis is the Deborah number, *De*, defined in the text, which is the ratio of the viscoelastic relaxation time of the matrix, τ, to the characteristic timescale of observation of the melt migration process, τ_{vw}. If the characteristic time is less than the relaxation time, then the effective matrix rheology response to the strains associated with melt migration will be elastic. The vertical axis is the Φg number, which is the ratio of the melt's gravitational energy release to the matrix's strain energy release during melt migration. Previous theories for melt migration in the crust and mantle have mainly considered the buoyancy of melt as the driving force for long-distance melt transport. In contrast, the vug wave theory considers matrix deformation to be a significant driving force for both fluid transport and segregation. The melt migration mechanism cartoons in this figure represent (a) porous flow and porosity waves, (b) tensile dike propagation, (c) vug waves, and (d) melt-rich networks formed by shear stress-driven segregation.

mechanisms [e.g., *Holtzman et al.*, 2003] and in models with continuum-mechanical compaction theory [e.g., *Stevenson*, 1989]. Here, we present a simple analytical model for a mechanism in which the matrix deforms elastically, representing the elastic end-member process on a continuum of viscoelasticity, as represented by the bottom axis of Figure 1.

[3] During porous flow, the migrating melt is assumed to form an interconnected network of grain-boundary tubules or macroscopic veins (or both) through which it can flow like water through a saturated sponge. The melt ascends if buoyant; its flow can also be influenced by large-scale pressure gradients due to plate spreading or subduction zone flow geometry [*Phipps Morgan*, 1987; *Spiegelman and McKenzie*, 1987] and anisotropic permeability arising from deformation of the surrounding matrix [*Phipps Morgan*, 1987; *Daines and Kohlstedt*, 1997; *Holtzman et al.*, 2003]. During tensile dike migration, the magma is assumed to be a buoyant fluid moving within a growing crack. For a typical magma-rock density contrast of 300 kg/m^3, the length of a vertical crack must exceed 100 m (its "Weertman length" [*Rubin*, 1998]), before it can spontaneously rupture at its tip and ascend [*Weertman*, 1971; *Rubin*, 1998]. Stresses arising from matrix deformation only influence the direction of dike ascent through changing the orientation of the maximum tensile stress [*Sleep*, 1984]. The migration trajectories of fluid-filled tensile cracks have been recently explored with both analogue [*Takada*, 1990; *Heimpel and Olson*, 1994] and numerical [*Dahm*, 2000] experiments, but these studies did not explore the small crack length and finite shear deformation region of parameter space in which "Weertman dikes" would not move, yet vug waves might stably propagate.

[4] Another important branch of research into the melt-migration problem considers the role of melt-rock disequilibria and dissolution-driven segregation [e.g., *Aharonov et al.*, 1995]. In these models, melt transport is driven by melt buoyancy and pressure gradients, while segregation into channels is driven by a dissolution-transport instability in which the local dissolution of pyroxenes by local melt-rock interaction increases permeability, concentrating local flow. That this mechanism occurs at mid-ocean ridges is supported by observations of the distribution and chemistry of dunites in the Oman and other ophiolites [e.g., *Braun and Kelemen*, 2002]. It is not yet known how this process compares kinetically with melt segregation/migration mechanisms other than viscous compaction, and over what depth-range it plays a significant role in shaping melt transport.

[5] Note the limited role of matrix deformation in shaping the above fluid transport mechanisms; in all of these fluid transport can occur in the absence of large-scale matrix deformation. Here we consider the "elastic" end-member example of a possible class of mechanisms for fluid migration in which matrix deformation is the primary force driving fluid migration. The fluid migrates as a means of reducing the internal strain energy of the matrix; in other words, the fluid migration is the primary agent of

Table 1. List of Symbols

Symbol	Meaning	Unit
τ_η	viscoelastic relaxation time	s
τ_{vw}	characteristic timescale of the vug wave process	s
u_{vw}	velocity of a vug wave	m/s
δ	"dislocation" displacement vector	m
$\overline{w}$	average width of the crack	m
l	length of the crack	m
η_f	viscosity of fluid in crack (1–10 Pa s, for slab interface and ridge, respectively)	Pa s
η	effective shear viscosity of the solid	Pa s
E	Young's Modulus (100 GPa for olivine)	Pa
De	Deborah number	–
G_I	normal strain energy release	J/m^2
G_{II}	shear strain energy release	J/m^2
$\dot{\Phi}_I$	normal strain energy release rate	W
$\dot{\Phi}_{II}$	shear strain energy release rate	W
ν_E	Poisson's ratio	–
μ_E	shear modulus (60 GPa for olivine)	P
$\Delta\sigma$	shear stress	Pa
$\Delta\rho$	density difference between melt and solid (300 kg/m^3)	kg/m^3
K_I	stress intensity factor, mode I	Pa $\sqrt{m}$
K_{II}	stress intensity factor, mode II	Pa $\sqrt{m}$
$\overline{P}$	mean overpressure ($P_{melt} - P_{lithostatic}$)	Pa
δP	pressure difference across length of crack	Pa
$\dot{\varphi}$	viscous energy dissipation in the crack-filling fluid	W
Φg	"Fiji" number, relates rate of shear strain energy release to gravitational energy release	–

matrix deformation. We shall analyze the simplest case of coupled matrix deformation and melt migration. We call the penny-shaped, fluid-filled crack dislocation a "vug wave." Vug is a Cornish word for a hole within the Earth (*Oxford English Dictionary*); "wave" was chosen to convey the idea that this deformation mechanism involves the migration of fluid-filled vugs through the rock: migrating penny-shaped, fluid-filled, self-healing crack dislocations. After developing an analytical theory of vug wave energetics, we will then examine its implications for melt migration and deformation in a range of geologic settings.

1.1. Recent Related Ideas in Physics and Geophysics

[6] Ideas that share some of the vug wave concept have been recently presented to explain the origin of friction and the earthquake slip process. Analogue experiments on the dynamics of sliding two foam blocks past each other [*Brune et al.*, 1989, 1993] suggested that the key to the relatively low-strength earthquake slip is the generation of a transient dynamically stable open and self-healing crack on the interface of earthquake rupture [*Brune et al.*, 1993; *Heaton*, 1990]. This research pursued ideas arising from earlier work by *Tolstoi* [1967] and *Shallamach* [1971] on the importance of dynamic vibrations for frictional slip of rubber and other solids. Recent numerical experiments on the origin of a frictional contact surface between two elastic bodies have led to the analogous proposal that the formation and seismic-slip propagation of self-sealing microcracks at the contact surface between two elastic blocks is responsible for the basic friction process itself [*Gerde and Marder*, 2001]. The vug wave concept differs from all of these previous ideas in two basic aspects: (1) the vug crack is fluid-filled instead of an open void, so that normal stresses can be continuous across the vug crack surface. (2) Because of the (relatively!) smaller viscosity contrast between melt and a viscoelastic matrix, a vug wave can move "slowly," stably propagating in the absence of inertial (i.e., seismic) forces. We anticipate that people will find a full spectrum of behavior between slow vug wave propagation and elastodynamic fracture processes.

2. Analytical Theory of Vug Wave Dynamics

2.1. Approximations

[7] To analyze the dynamics of vug waves in a simple form, we make the following approximations:

[8] 1. The matrix deforms elastically. The elastic approximation to a viscoelastic rheology is well-founded if the timescale for vug wave propagation is short compared to the Maxwell relaxation time of the viscoelastic matrix. Below, we demonstrate that this criteria is well met. In order for the elastic end-member analysis to be valid for a viscoelastic solid such as the mantle, the characteristic timescale for the vug wave process, τ_{vw}, must be shorter than the mantle's local viscoelastic relaxation time,

$$\tau_\eta = 2\eta_s/E, \quad (1)$$

where η is the mantle's shear viscosity and its elastic modulus ($\approx 10^{11}$ Pa). Symbols are defined in Table 1. The relationship between the timescales of vug wave motion and viscous mantle relaxation is described by a dimensionless "Deborah number,"

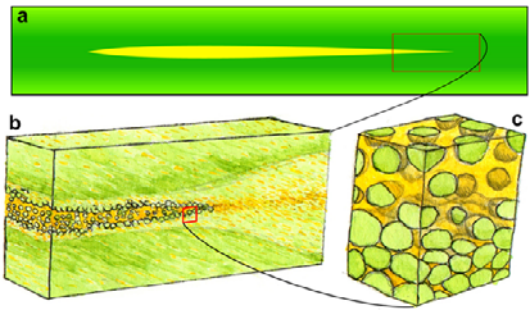

Figure 2. Vug wave end-members. (a) In an idealized vug wave in a predominantly elastic matrix ($De \gg 1$), fracture tips cut through the grains of an effectively melt-free matrix. (b) In another possible end-member, the poroviscoelastic properties of the matrix are important ($De \geq 1$), and the wave behavior arises when the effect of a rheologically critical melt fraction is surpassed in the vug region. In this case a vug wave in the mantle is similar to a porosity wave driven by shear stress, in that its tip is marked by a local increase in melt fraction. However, in a vug wave, farther from the tip, the melt fraction surpasses the rheologically critical melt fraction, and the melt-crystal mixture in the cavity deforms as a weak viscous fluid instead a solid.

De. The relaxation time for the mantle is ≈3 years for a shear viscosity of 10^{19} Pa s. We define the characteristic timescale for the vug wave movement as the time required for a wave to move over one crack length, essentially the time during which it interacts with the rock through which it passes. This characteristic timescale $\tau_{vw} = u_{vw}/l$, where l is the length and u_{vw} is the velocity of a vug wave. For the situations considered in this paper, this elastic timescale approximation is well-satisfied.

[9] 2. The vug is assumed to be a crack-like feature, specifically a 2-D crack. This assumption is clearly oversimplified as the problem is not 2-D. We envision each vug wave is physically a three-dimensional "penny-shaped" crack [*Broek*, 1987, p. 88] within the matrix, yet because 2-D fracture theory has a rich array of useful analytical solutions, we use this assumption common to previous studies of dike ascent through the mantle [e.g., *Weertman*, 1971; *Spence and Turcotte*, 1990; *Rubin*, 1998].

[10] 3. The vug fluid is assumed to be a Newtonian viscous fluid. Because the vug is "crack-like," lubrication theory approximations are used to simplify the flow solution for viscous flow in a thin crack following the approach of previous workers [*Spence and Turcotte*, 1990; *Rubin*, 1998]. Note that the key aspect of this approximation is that the material within the vug deforms much more readily than its surroundings, which can also occur if the vug fluid is created by a process that causes the vug-filling material to exceed the "rheologically critical melt fraction" (RCMF) [*Renner et al.*, 2000]. The RMCF is defined as the threshold melt fraction at which a partially molten assemblage changes rheology from a "solid" dominated by the mechanical properties of the matrix to a much weaker "fluid" dominated by the mechanical properties of the interstitial melt phase. This transition is further discussed in section 3.2.

[11] 4. For calculating the flow of the vug fluid, the vug is assumed to be a constant thickness crack of average width $\bar{w}$. This last approximation allows a simple analytical solution for the flow within a crack.

[12] 5. The crack preserves its shape (i.e., we will search for and find a self-similar solution). The last two assumptions have the merit that they allow the following simple energy-based analysis of vug wave propagation. After developing and presenting the simple theory that emerges from these assumptions, we will discuss their physical implications and incompleteness when discussing possible "closure" processes for the migrating vug wave tail.

[13] In calling the vug wave a migrating crack, we are making a great simplification; in reality, we view this process as the movement of any concentration of melt driven by shear. The behavior of the matrix may be defined as a spectrum, with elastic and viscous end-members, as represented by the bottom row of Figure 1. (1) In the elastic case, a true fracture would propagate through a poroelastic medium and perfectly seal at its tail. (2) In the viscous case, the wave is simply a high concentration of magma (near or above the RCMF) in a viscous matrix driven by shear stress instead of the usual buoyancy. The viscous end-member is not described by the following equations, but we do discuss how far into the viscoelastic realm the following equations may have validity. In high-temperature, partially molten conditions a range of mechanisms may exist that could relax the stress concentrations at the front of the vug wave, such as small-scale diffusion or dislocation creep and surface tension-driven dispersion of melt by local porous flow. Another likely scenario is that melt migrates locally by porous flow toward the underpressured tip and causes grain disaggregation as the RCMF is surpassed; this concentration process is the propagation of the vug tip. In this view, as illustrated in Figure 2, the complete propagation of

a vug wave involves the conversion of a partially molten rock to a suspension of crystals in magma at the propagating tip of the vug wave, with the reconversion to a matrix-supported partially molten solid at the tail. In this sense, the movement of a vug wave is similar to the propagation of a porosity wave that is driven by the strain-energy release associated with matrix deformation. In this paper, we avoid the wide range of complexity in these differing physical scenarios, to present the idea in its simplest, elastic-fracture form.

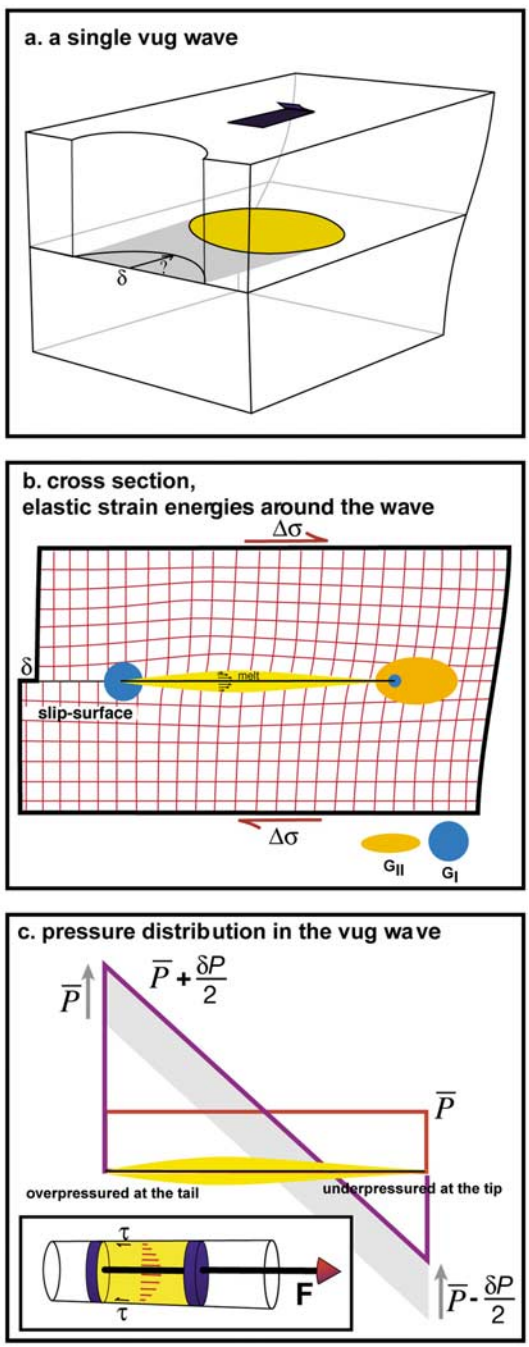

2.2. Analytic Solutions

[14] Conceptually similar to a dislocation, a vug wave moves as the agent of matrix deformation. Nondilatent (constant volume) motion of a vug wave involves breaking a new crack surface at the tip of the migrating fluid-filled vug dislocation, and closing the tail while preserving the matrix shear slip that occurs across the fluid, as illustrated in Figure 3a. In this case the matrix releases shear strain energy as the vug wave moves; the region of high elastic strain energy advances forward into the unslipped part of the matrix, and the vug wave follows in its wake.

[15] In two dimensions, i.e., assuming a crack geometry that is infinitely long in the out-of-plane direction, analytical expressions are known for these crack energetics. (The book by *Lawn* [1993] provides a good introduction to the subject of fracture mechanics, while *Tada et al.* [1973] is a compendium of analytical solutions.) The mode II (shear) energy release, G_{II}^{tip}, per unit length of vug wave propagation is calculated assuming that the dislocation is zero at the crack tip ($x = l$), and reaches its maximum (permanent) slip at the crack's tail ($x = 0$). This shear strain energy release is given by G_{II}^{tip} for the tip of a shear crack of length $2l$ [*Tada et al.*, 1973, p. 1.8]:

$$G_{II}^{tip} = \frac{1-\nu_E}{2\mu_E} K_{II}^2 = \frac{\pi(1-\nu_E)}{2\mu_E} (\Delta\sigma)^2 l, \qquad (2)$$

Figure 3. Vug wave mechanics. (a) An ideal vug wave has a disc shape and moves in the shear direction along a shear plane. The "dislocation displacement" vector δ is longest in the middle of the vug wave. (b) Elastic strain energies both drive and resist vug wave movement. The orange oval represents shear (mode II) strain energy; the blue circle represents tensile (mode I) strain energy. There is no shear strain energy in the tail because the matrix can slip in shear across the fluid in the crack; in turn, viscous dissipation within the fluid resists vug wave movement. As discussed in the text, during steady-state vug wave motion, the viscous dissipation to move the vug fluid and the net mode I elastic strain energy consumed in opening and shutting the crack both resist vug wave motion. (c) The pressure distribution in a vug wave can be separated into two contributions: (1) a net mean overpressure, $\overline{P}$, and (2) the along-crack pressure gradient, $\delta P/l$. The inset shows the origin of the dynamic along-crack pressure gradient that is created by movement of the constant-volume vug crack.

where the shear stress $\Delta\sigma = \sigma_{Far} - \sigma_{vug-wall} \approx \sigma_{Far}$ (i.e., assuming the fluid-filled crack cannot sustain a sizable shear stress across it), ν_E is Poisson's ratio, K_{II} is the mode II stress intensity factor or fracture toughness (a measure of the energy consumed in forming a new surface at the growing tip), and μ_E is the shear modulus of the medium through which the vug wave propagates. The 2-D geometry of the idealized vug wave (VW) is shown in Figure 3b. Because the tail end of the VW incorporates a permanent slip dislocation, its offset and stress are equivalent to the offset and stress at the midpoint of an isolated shear crack of twice the length in the same regional stress field. For crack motion at a speed u, the net rate of G_{II}^{tip} energy release is

$$\dot{\Phi}_{II} = \frac{\pi(1-\nu_E)}{2\mu_E}(\Delta\sigma)^2 lu. \tag{3}$$

Vug wave ascent also leads to a reduction in gravitational energy (the equivalent to a buoyancy force when considering energetics). This driving term is typically small in comparison to the reduction in strain energy (as will be discussed in a later section), but still plays an important role in favoring buoyant ascent over descent. For ascent at an angle θ from the vertical, the rate of gravitational energy release from a vug wave of mean width $\bar{w}$ is

$$\dot{\Phi}_{grav} = u\Delta\rho g l \bar{w}\cos\theta, \tag{4}$$

where $\Delta\rho = \rho_{melt} - \rho_{matrix}$.

[16] In order for the fluid to flow into the growing tip, it must be an open crack (mode I). Pressure within the fluid must drive crack-tip opening; the along-crack pressure can be described as the combination of a mean overpressure and a pressure gradient, illustrated in Figure 3c. Tip opening and tail closing during vug wave motion consumes net mode I strain energy. (We will later find that tip opening and tail closing consumes two thirds of the mode II strain energy liberated by vug wave motion, with the rest of the energy primarily consumed by viscous dissipation linked to moving the fluid within the moving crack.) The net mode I strain-energy consumption $G_I^{tip} - G_I^{tail}$ is found by using the solutions for the tip- and tail-stress intensity factors for a crack with a linearly varying crack pressure along its length [*Tada et al.*, 1973, p. 5.13]. A constant along-crack pressure gradient is that needed to move the fluid through a constant thickness crack as shown in Figure 2c:

$$\begin{aligned} G_I^{tip} - G_I^{tail} &= \frac{1-\nu_E}{2\mu_E}\left\{\left(K_I^{tip}\right)^2 - \left(K_I^{tail}\right)^2\right\} \\ &= -\frac{\pi(1-\nu_E)}{2\mu_E}\bar{P}\delta P l, \end{aligned} \tag{5}$$

where $\bar{P}$ is the mean vug crack overpressure, $\delta P/l$ is the along-crack pressure gradient, and l, ν_E, and μ_E are defined above. This equation describes the difference in energy consumption between opening the tip and closing the tail of the crack. For a vug wave moving at speed u, this implies a net mode I energy consumption rate (where the minus sign reflects "consumption")

$$\dot{\Phi}_I = -\frac{\pi(1-\nu_E)}{2\mu_E}\bar{P}\delta P l u. \tag{6}$$

[17] There are two additional sources of resistance to vug wave motion: (1) the fluid must move as the vug wave moves (which induces viscous dissipation within the moving fluid), and (2) a new shear crack surface must be formed at the growing vug tip (fracture toughness).

[18] 1. The viscous dissipation in the moving fluid within the vug controls the speed of the vug wave migration and determines the along-crack pressure gradients within the moving vug wave, as shown in Figure 3c. To estimate viscous dissipation, we approximate the vug as a crack of constant width (or thickness) $\bar{w}$ that for an overpressured mode I crack can be expressed in terms of the mean overpressure $\bar{P}$ and crack length l as

$$\bar{w} = (\pi/4)\frac{(1-\nu_E)}{\mu_E}\bar{P}l. \tag{7}$$

For this geometry, the viscous dissipation $\dot{\varphi}$ is

$$\dot{\varphi} = -12\eta_f \frac{l}{\bar{w}}u^2, \tag{8}$$

where u is the average flow rate through the crack. This relation for viscous dissipation is based on the channel (Poiseuille) flow solution through a 2-D channel of constant width [*Turcotte and Schubert*, 1982, p. 234], in which the local viscous dissipation per unit crack length is equal to the product of the local along-crack pressure gradient dP/ds times the net fluid flux (mean velocity times crack width) through the crack. Since the volume of the crack is constant,

movement of the tip exerts a pull on the fluid, inducing an along-crack pressure gradient

$$dP/ds = 12\eta_f u/\bar{w}^2, \quad (9)$$

where the vug tip is a pressure low and the vug tail is a pressure high. (Note that a solution for D'Arcy-flow-like migration of melt in a "porous" high-permeability vug crack would lead to a similar parametric relation between the along-crack pressure distribution and fluid transport.)

[19] 2. The fracture toughness associated with creating the new shear crack tip surface area [*Atkinson and Meredith*, 1987; *Rubin*, 1998]

$$G_{II}^{tip-yield} = -\frac{(1-\nu_E)}{2\mu_E}\left(K_{II}^{yield}\right)^2. \quad (10)$$

A value of $K_{II}^{yield} = 3$ MPa $\sqrt{m}$ for the formation of new surfaces in olivine [*Atkinson and Meredith*, 1987] leads to a rate of energy consumption

$$\dot{\Phi}_{II}^{tip-yield} = -9\left[\left(\mathrm{MPa}\sqrt{m}\right)^2\right]u\frac{(1-\nu_E)}{2\mu_E}. \quad (11)$$

This value is likely an upper limit for mantle processes, and it would be reduced by any stress-relaxation processes at the crack tip. The fracture toughness determines the smallest size at which a fluid-filled crack can move as a vug wave: $\frac{\pi(1-\nu_E)}{2\mu_R}(\Delta\sigma)^2 l$ must be larger than $\frac{9\left[(MPa\sqrt{m})^2\right](1-\nu_E)}{2\mu_E}$. (For a regional far-field deviatoric stress of 1 MPa, this minimum size is ≈3 m.)

[20] Combining equations (3), (4), (6), (8) and (11) into a single expression leads to the following net work balance associated with the stable migration of a vug wave:

$$\left[\dot{\Phi}_{II}\right] + \dot{\Phi}_{grav} + \left[\dot{\Phi}_I\right] + [\dot{\varphi}] + \dot{\Phi}_{II}^{tip-yield} = 0, \quad (12)$$

where the first two terms in this equation represent net energy releases driving vug wave propagation, and the last three terms are energy sinks that resist its migration.

2.3. Speed of Vug Wave Propagation (in the Elastic Limit)

[21] For vug waves of length 10–1000 m, the dominant driving and resisting terms are the terms highlighted with brackets in equation (12): mode II strain-energy release (proportional to the vug wave speed) is what drives vug wave motion; mode I strain-energy consumption (proportional to the square of the speed), and viscous dissipation associated with vug wave motion (also proportional to the square of the speed) are what limit how fast the vug wave will move. The energy analysis including only these three dominant terms predicts the speed for stable vug wave propagation:

$$u = \frac{\pi^2(1-\nu_E)^2\bar{P}(\Delta\sigma)^2 l}{288\mu_E^2\eta_f} \quad (13)$$

or

$$u = \frac{\pi^2(1-\nu_E)^2\bar{P}^2(\delta P) l}{192\mu_E^2\eta_f} \quad (14)$$

(the two forms are equivalent), plotted in Figure 4a. Velocity is proportional to the square of the far-field stress, and linearly proportional to the length and the overpressure. (The relation $(\Delta\sigma)^2 = (3/2)\bar{P}\delta P$ can be seen either from the equivalence of (13) and (14) or directly from the expressions (3) and (6) and the relation that the viscous dissipation is equal to half of (6).)

[22] In the above analysis, the elastic resistance to vug wave motion is twice as large as the viscous resistance (the viscous dissipation within the vug fluid is half the elastic strain-energy reduction between opening the tip and closing the tail), and one third of the shear-strain energy release goes into heating the vug fluid. This can be seen by rewriting (9) as $\delta P = 12\ \eta_f u l/\bar{w}^2$ and substituting this relation into (8), which results in $\dot{\varphi} = -\delta P\bar{w}u$. Further substitution of (7) for $\bar{w}$ leads to $\dot{\varphi} = \dot{\Phi}_I/2$.

2.4. Criterion for the Validity of the Elastic Solution: The *De* Number

[23] Here, we assess several simple criteria to decide how appropriate this elastic solution is in a viscoelastic world. As discussed in section 2.1, the first order estimate of the validity of the solution is to calculate the Deborah number [e.g., *Connolly and Podladchikov*, 1998]. The local viscoelastic relaxation time of the upper mantle from equation (1) is 0.6 to 60 years for Newtonian viscosities of 10^{18} to 10^{20} respectively. For a vug wave, the characteristic time, τ_{vw}, is the length of time that any portion of rock will interact with a particular passing fracture, which is simply

$$\tau_{vw} = l/u_{vw} \approx \frac{29\eta_f}{\bar{P}(\Delta\sigma)^2}\left(\frac{\mu}{1-\nu}\right)^2, \quad (15)$$

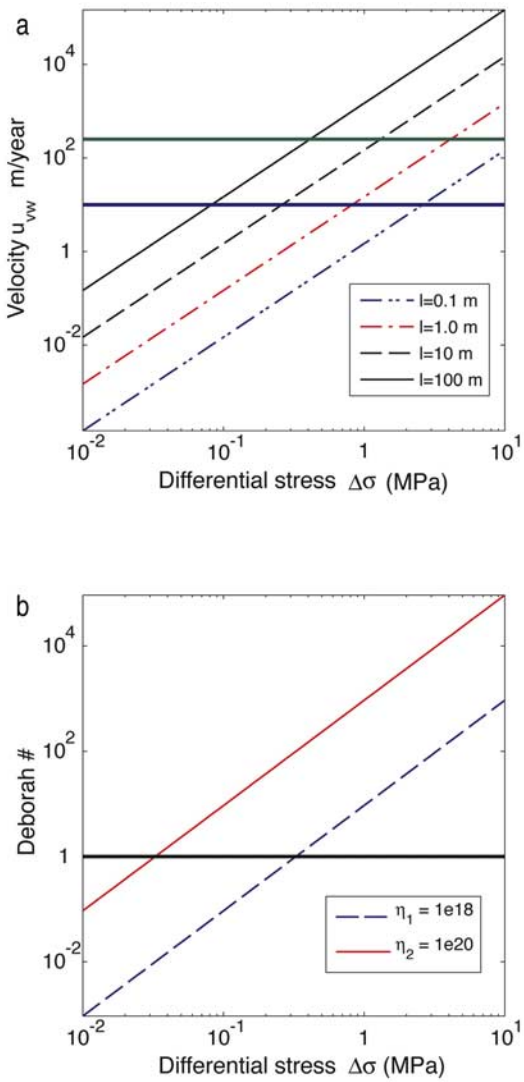

Figure 4. Solutions for vug wave velocity in the elastic limit. (a) Velocity as a function of far-field stress and vug wave length. The speed increases with longer waves and higher stress. The two horizontal lines mark constraints on the fastest melt migration beneath the ridge, which vug waves can fairly easily satisfy in the elastic limit, with the caveats discussed in the text. (b) Deborah number as a function of stress and mantle viscosity. For reasonable values of mantle stress and viscosity, $De \gg 1$, a necessary (but not sufficient) condition for the validity of the elastic solution.

and so

$$De = \frac{\tau_\eta}{\tau_{vw}} = \frac{2\eta_s}{E\tau_{vw}} \approx \frac{\bar{P}(\Delta\sigma)^2\eta_s}{15E\eta_f}\left(\frac{1-\nu}{\mu}\right)^2. \qquad (16)$$

[24] In the simple formulation above, because the velocity is linearly dependent on the length of the crack, the characteristic timescale is independent of crack length. *De* is plotted in Figure 4b. When $\bar{P}$ = $\Delta\sigma$ = 1 MPa, and mantle viscosities of 10^{18} Pa s to 10^{20} Pa s, as above, *De* = 10 and 1000, respectively. When $De \gg 1$, the elastic approximation is reasonable. As shown in Figure 4b, the elastic solution is reasonable for mantle conditions when $\bar{P} > 1$ MPa, and $\Delta\sigma > 0.1$ MPa. The latter is a very reasonable value for mantle shear stresses. The origin of the overpressure will be discussed below.

[25] This criterion becomes much more complicated when one considers stress relaxation by viscous creep processes. At high-temperature, partially molten conditions of the asthenosphere, such relaxation at the grain scale is likely to be important and may significantly reduce the stress intensity at the crack tip, reducing the viability and the velocity of the vug wave. Specifically, the velocity of a fracture tip in the presence of creep-relaxation processes is a power-law function of velocity of the crack: the faster the crack-tip velocity, the higher the stress intensity associated with crack-tip propagation [e.g., *Lobkovsky and Langer*, 1998; *Pegoretti and Ricco*, 2001]. This relation introduces a nonlinearity into these equations, a complication we leave for future study.

2.5. Relative Importance of Strain Energy Release Versus Buoyancy: The Φ*g* Number

[26] In this theory, whether melt propagates as a vug wave or tensile dike will depend on the relative importance of the release of strain energy versus gravitational energy (buoyancy). The elastic shear strain-energy release Φ_{II} per unit distance of vug wave migration is

$$\Phi_{II} = \frac{\pi(1-\upsilon_E)(\Delta\sigma)^2 l}{2\mu_E}, \qquad (17)$$

while the gravitational energy release (assuming that the vug wave migrates at an angle θ from the vertical) is

$$\Phi_{grav} = \frac{\pi(1-\upsilon_E)\Delta\rho g l^2 \bar{P}\cos\theta}{4\mu_E}. \qquad (18)$$

We call the dimensionless ratio of these two energy releases the Φ*g* number (sounds like "Fiji"):

$$\Phi g = \frac{2(\Delta\sigma)^2}{\Delta\rho g l \bar{P}\cos\theta}. \qquad (19)$$

Φ*g* = 100 for a vug wave with *l* = 10 m, $\bar{P}$ = $\Delta\sigma$ = 1 MPa cos θ = 1 (vertical ascent), and $\Delta\rho$ = 300 kg/m^3. For this melt-rock density contrast, only for vug waves more than a kilometer in

length would the gravitational energy release be larger than the shear strain energy release associated with vug wave propagation (i.e., for $l >$ 1 km, $\Phi g < 1$). Thus there appears to be a significant intermediate length-scale in which rock deformation should play a more important role than magma buoyancy in driving magma migration.

3. Discussion

3.1. Limits of the Current, Energetics-Based Theory

[27] When applicable, energy arguments often lead to simple and powerful theoretical formulations that bypass the considerable mathematical complexity of problems combining elasticity, fracture, and viscous flow. The above analysis showed that vug wave propagation is energetically feasible, and could determine the speed of such vug wave propagation if it does occur. However, this is not the same as demonstrating that vug wave behavior does occur; to do so, we will need either a more complete theory or a convincing laboratory demonstration. Here, we discuss more of the realistic complexity of the problem.

3.2. Vug Wave Nucleation and the Origin of Melt Overpressure $\bar{P}$

[28] We envision that vug wave nucleation requires both an ambient melt overpressure (which may be quite small) and the presence of planar concentrations of melt. Such planar concentrations of melt can form in several ways, driven by reactive instabilities [e.g., *Aharonov et al.*, 1995] and/or by shear stress in the parameter regime where local viscous matrix deformation dominates melt buoyancy as the driving force for melt migration [e.g., *Holtzman et al.*, 2003]. The necessary melt overpressure (1 MPa was assumed in the previous analysis) appears easy to achieve as this overpressure is routinely found in dynamic poroviscous melt migration calculations [*Aharonov et al.*, 1995; *Connolly and Podladchikov*, 1998; *Kelemen et al.*, 1997], and is also the overpressure that would be generated by the intrinsic volume increase between melt and solid produced by a 50 m interval of pressure-release melting prior to melt escape (see Appendix A). For a more complicated scenario, *Renner et al.* [2000] demonstrated that during deformation of a partially molten solid the overpressure depends on the permeability, i.e., on how rapidly melt can escape or reorganize. Thus, when shear is localized in weak, melt-rich layers, the melt may experience a slight overpressure if it cannot escape quickly enough to relax the mean stress in the solid matrix.

[29] During the nucleation stage of a vug wave, growth of one end of the proto shear crack would release more energy than the growth of the other, for example because its extension would be upward (releasing more gravitational energy) or into the direction of increasing shear stress (releasing more shear-strain energy). This second order asymmetry in the energy release associated with crack growth is what would favor initial growth of one crack tip over the other. The dynamics of this transient start-up phase are not analyzed in this study, which focuses on the easier-to-address question of whether and how a vug wave, once formed, would stably migrate.

3.3. Crack Closure Problem

[30] The biggest uncertainties in the above formulation arise from the coupling of viscous flow within a thin crack and elastic crack theory. We have assumed (like many previous workers, from *Weertman* [1971] to *Dahm* [2000]) that the vug crack tail closes, but the details of how it closes cannot be found from these simple energy-based arguments. For example, *Stevenson* [1983] noted that there is an inherent inconsistency in coupling tensile crack growth to viscous flow within these cracks; as the crack thins, it becomes harder and harder for viscous pressure gradients to squeeze melt in or out of it, because the necessary pressure gradient depends on the inverse cube of the crack width. The physical meaning of this relation is unclear; in the field one often sees ''ends'' to dikes, which indicates that nature does not suffer (as much as we do) from our conceptual difficulties.

[31] We see several possible mechanisms to close the tail:

[32] 1. First, if the vug wave leaves behind it a thin film of melt, that melt will be quickly disseminated into nearby triple and quadruple junctions by surface tension, which is possible when the melt tends to wet grain boundaries, as in the olivine + basalt system [e.g., *Stevenson*, 1986; *Riley and Kohlstedt*, 1991]. This force can be quite large between geologically immiscible materials such as a vapor, an aqueous, or a molten-iron vug fluid and its silicate host but is significantly smaller between basaltic magmas and solid peridotite.

[33] 2. If a vug wave is propagating through a porous elastic or viscoelastic matrix, melt or fluid may be pulled in at the tip and expelled at the tail. In this scenario, based on the one discussed in section 2.1 and Figure 2b, the "crack" is that region which has surpassed the threshold melt fraction, known as the rheologically critical melt fraction (RCMF). Thus, to close, the melt fraction simply has to descend below the RCMF as melt is expelled toward the direction of propagation. Some of that melt may also be injected back into the matrix and disseminated by surface tension as discussed above. However, because permeability generally depends strongly on melt fraction, it may be easier to pull melt into the crack near the propagating crack tip than to reinject it into the matrix near the crack tail. In this case, the crack volume will grow. Because velocity depends on length, as it grows it may also accelerate. In this scenario, *Stevenson*'s [1983] objection is no longer applicable, as one would simply be using idealized "elastic crack" and "viscous flow within a crack' approximations to describe the solid" and "fluid" end-member behaviors of this well-defined (but more complex!) material. The previous two possibilities deserve in-depth numerical exploration with variants of the numeric approach of *Connolly and Podladchikov* [1998] that can incorporate boundary conditions of simple shear deformation.

[34] 3. If the vug wave propagates through a region that is partially molten, the higher pressure within the vug tail could promote freezing (crystal growth) just as the low-pressure tip promotes partial melting of the surrounding host rock, which could also provide a possible thermodynamic mechanism for tail closure. Exploring this idea would require development of a coupled thermodynamic-mechanical approach (e.g., latent heat effects and local heat conduction can become locally important), and may suggest field-observational tests. While each of these possible mechanisms may be applicable under certain conditions, we do not yet see a better way to incorporate any into the previous, simple energy-based theoretical derivation.

4. Applications

[35] The potential applications to nature are numerous. Such a simple theory may be easily adapted to a wide range of fluid-rich rapidly deforming settings in the earth. We focus our discussion on one possible application of vug waves to a particularly exciting discovery in geodynamics, and conclude with a short list of several other possible applications.

4.1. Vug Waves and "Silent Slip"

[36] Great insight into the dynamics of subduction zones may soon come from recent observations of short lurches in crustal movements associated with quiet seismic rumbling. In Cascadia, GPS stations generally migrate monotonously landward, punctuated by brief lurches of 2 mm seaward over a period of 10 days. These lurches are associated with very subdued seismic rumbling or noise, but no marked "normal" seismicity. *Dragert et al.* [2001] estimate that the slip process responsible for the lurches occurred over an area of about 50 km (in the subduction direction) by 300 km (trench parallel) on the slab-mantle wedge interface, based on the distribution of the GPS stations at which the movements are observed. This patch of the interface occurs at depths of about 30–40 km, which they estimate corresponds to temperatures of about 500°C. Furthermore, the lurches are periodic, occurring about every 13–16 months [*Dragert et al.*, 2004]. Similar phenomena are occurring in other subduction zones in Japan [e.g., *Ozawa et al.*, 2001] and Mexico [e.g., *Lowry et al.*, 2001]. Thus this phenomenon, referred to as "silent slip" or episodic tremor and slip (ETS) may be a common part of the subduction process and tell us a great deal about the processes of coupled fluid flow and rock deformation in general.

[37] Here, we suggest that silent slip may be explained by a vug wave mechanism. The slip must occur by a sudden change in the effective rheological properties of the interface, and the mechanism must be able to explain the observed periodicity, velocity, and aseismicity. If a dislocation-like process is responsible for the slip, the velocity of the vug wave is much faster than the plate velocity; it is roughly the up-dip length of the slipping patch divided by the duration of the event: 50 km/10 days or 0.06 m/s. Thus we imagine that fleets of vug waves migrate up the slope of the interface at roughly this velocity, transporting fluid in them, as shown in Figure 5. This velocity is within the realm of possibility as predicted from the simple analysis here, using parameters of $l = 1–100$ m, $\Delta\sigma = 1–100$ MPa, $\bar{P} = 1$ MPa, $\eta_f = 1$ Pa s (for a "wet" melt) and $\mu = 60$ GPa, as shown in Figure 6. Note that if η_f is that of an aqueous fluid ($\sim$0.01 Pa s), then much smaller waves will be able to achieve the required velocities. Even if the temperatures are warmer than suggested (500°C), the elastic end-

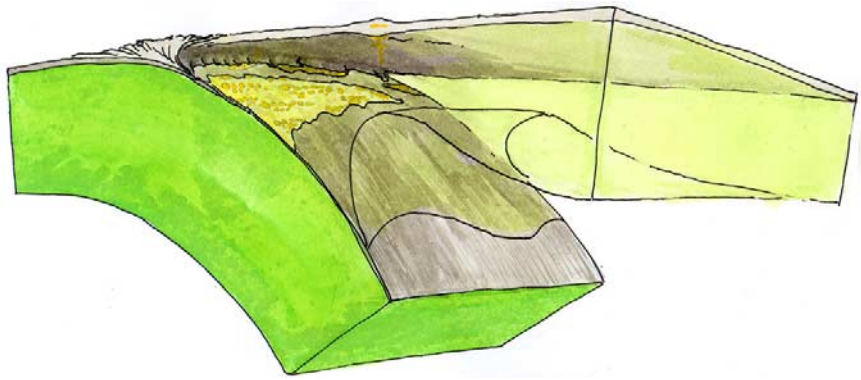

Figure 5. Vug waves as agents of "silent slip." This sketch depicts fleets of vug waves creeping up the slab interface toward the locked zone of the interface between two plates. The whitish area with yellow dots signifies the region where episodic tremor and slip (ETS) originates [*Dragert et al.*, 2001], with the migration of clusters of vug waves as the physical mechanism for the subseismic displacements.

member analysis may be reasonable because crack-tip relaxation would probably be quite slow. The viscosity of damp olivine aggregates in the mantle wedge would be $\approx 10^{21}$ Pa s and in the slab at 900°C, $>10^{22}$ Pa s at 50 km [*Hirth and Kohlstedt*, 2004]. Taking these as extreme lower bound estimates, considering the estimate of 500°C, the viscoelastic relaxation times would still be 500 and 5000 years, respectively, much longer than the characteristic timescale of the slip process.

[38] The periodicity may reflect the time required for sufficient fluid volume and fluid pressure to accumulate, and for sufficient elastic strain to produce the required background stress to drive vug waves. The latter may be estimated in the following manner: after a stress-releasing event, stress in the region will accumulate to its background viscoelastic level (which is a function of the strain rate) in approximately the viscoelastic relaxation time. For $\eta_s = 10^{19}$ Pa s (a very low estimate for the slab-wedge interface), $\tau_\eta \approx 1$ year, on the same order as the periodicity of silent slip episodes. If the slab-wedge interface is 1 km thick accommodating a convergence rate of 3 cm/year, a strain rate of 10^{-12} s^{-1}, and the same viscosity will yield a stress of 10 MPa. The rate of fluid release and accumulation is more difficult to estimate. The region where the up-dip end of the slipped patch makes a transition to the beginning of the locked zone may occur where vug waves die; death may occur for several reasons: (1) the fluid freezes, (2) the surrounding rock begins to fracture by fluid overpressure and the fluid disperses in the medium.

[39] If the characteristic shear stress, $\Delta\sigma$, and/or vug wave overpressure, $\bar{P}$, can be better constrained, then one could further quantify the vug wave theory to relate the creep along a subduction zone to the fluid migration and effective rheology within this region. For example, the net slip rate along a fault surface deforming by vug wave passage along the fault would be equal to the slip-increment associated with each vug wave ($2(\Delta\sigma l/\mu_E(1 + \nu_E)$) multiplied by the number of vug waves that pass a point per unit time, while the fluid flux transported by these vug waves would be the cross-sectional area of a vug wave ($= l^2\bar{P}\frac{\pi}{4}\frac{(1-\nu)}{\mu_E}$) times the number of vug waves per unit time. This implies that the ratio of fluid transport to slip will

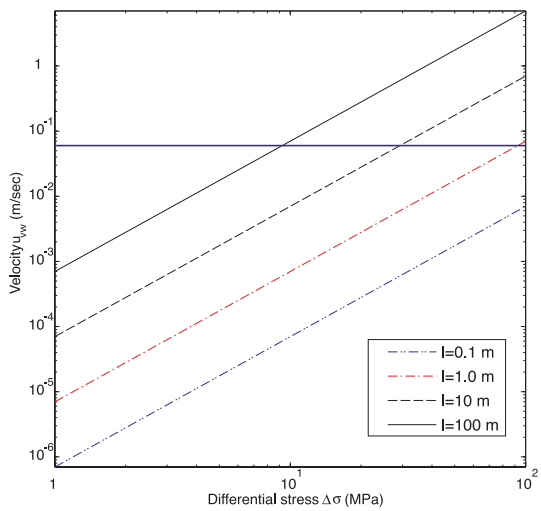

Figure 6. Vug wave velocities at conditions estimated for Cascadian episodic tremor and slip (ETS). The horizontal line represents "defect" velocities necessary for a dislocation-like process to account for displacement across the area estimated for the Cascadian ETS by *Dragert et al.* [2001]. These velocities appear easy to achieve based on the simple analysis presented in the text.

be $\approx 0.37 l\bar{P}/\Delta\sigma$, i.e., proportional to the characteristic length of a vug wave, and also proportional to the ratio of $\bar{P}$ to the characteristic shear stress in the region, $\Delta\sigma$. For small $\bar{P}/\Delta\sigma$ ratios, vug waves can lead to large deformations associated with relatively small fluid-transport. For example, if the $\bar{P}/\Delta\sigma$ ratio is 10^{-2}, then the propagation of a millions of 3-m-sized vug waves, each associated with $\approx$1 mm of slip, would lead to 1 km of slip for each 10 m^3/m of fluid transport per meter cross section along the fault surface.

4.2. Other Potential Applications

4.2.1. Ridge Melt Extraction

[40] Vug waves and their more viscous/viscoelastic variants may be important melt transport mechanisms beneath spreading centers. In the high-temperature, partially molten conditions of the upwelling asthenosphere, the vug wave may be closer to the viscous end-member discussed in section 2.1. In this case, a different set of equations will be required to estimate the velocity. Nonetheless, the concept may still be very relevant.

[41] Recent geochemical discoveries on trapped melt inclusions and short-lived radionucliides in mid-ocean ridge basalts (MORB) pose two fundamental problems for previous ideas for subaxial melt transport. Melt inclusions trapped in olivine xenocrysts indicate that many small and chemically distinct batches of melt may form and ascend at depth beneath a spreading center [*Sobolev and Shimizu*, 1993, 1994]. Short-lived radionucliide data indicates that magmas quickly ascend from regions of magma generation to surface eruption, spending less than 100–10,000 years in transit between melting at 25–100 km depth to volcanic eruption [*Sims et al.*, 2003; *Rubin*, 1998; *Goldstein et al.*, 1991; *Lundstrom et al.*, 1999]. These velocities, 10–250 m/yr, are marked on Figure 4a. Ascending vug waves can contribute to a solution for these observational constraints. By definition, vug waves move small batches of melt; the current form of the analysis suggests that a 10 m diameter, 1 mm thick melt "disc" can propagate as a vug wave for a melt overpressure and ambient deviatoric shear stress of 1 MPa. In the absence of viscous relaxation of crack-tip stresses, such vug wave would take only 1500 years to traverse the 100 km from source to surface. For a single vug wave, these equations would provide an upper-end estimate of the velocity. More rapid ascent may occur if small vug waves coalesce into larger, even faster moving ones.

[42] To imagine how vug waves may contribute to the melt transport process beneath a mid-ocean ridge, we return to the melt migration mechanism map in Figure 1. Generally, the melt migration process will move from predominantly viscous to elastic matrix control as temperature drops and as melts ascend. In Figure 1, the *De* number defined above forms the horizontal axis determining the relative importance of elastic versus viscous matrix deformation. On the vertical axis, the Φg number, also defined above, describes the competition between the two primary driving forces for melt migration, melt buoyancy and matrix strain-energy reduction. Many paths through the space defined in Figure 1 may be possible. For example, when high-productivity melting begins, melt may initially segregate into channels by stress-driven organization [e.g., *Holtzman et al.*, 2003]. In the higher stress/higher viscosity regions of the subridge environment these channels may degenerate into vug waves. When the matrix permeability becomes too high to maintain a the necessary overpressure, or when the ambient shear stress becomes too low to drive transport, then they may transform into buoyancy-driven porosity waves. When buoyancy forces become large relative to matrix strain energy reduction ($\Phi g < 1$), the vug waves may transform into tensile dikes or porosity waves. They can also stop if the fluid freezes. A third axis, not shown, describes the kinetics of melt-rock reaction which also may occur during vug wave migration.

[43] The vug wave mechanism also offers an attractive mechanism for focusing widely dispersed subaxial melts into the narrow axial neovolcanic zone observed at all spreading centers [*Phipps Morgan*, 1987; *Macdonald*, 1982]. For plate separating above a uniform viscosity asthenosphere substrate, planes of maximum shear stress point toward the spreading axis [*Phipps Morgan*, 1987]. The maximum shear stress increases toward the spreading axis as [*Phipps Morgan*, 1987]

$$\sigma_{r\theta} = (8\pi) U \eta_s \sin\theta / r, \tag{20}$$

where U is the half-spreading rate, η_s is the subridge asthenosphere viscosity, r is the radial distance from the spreading axis, and θ is the angle between this radius and a vertical line beneath the axis. The solution is plotted in Figure 7. It clearly shows that the stresses increase toward the sides

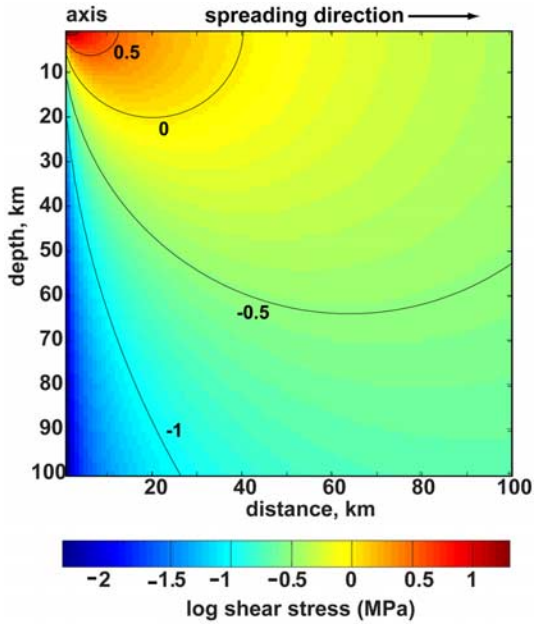

Figure 7. Corner-flow stress map. The distribution of shear stress beneath the ridge is calculated from an analytical solution to the plate spreading-driven corner flow beneath a ridge [*Phipps Morgan*, 1987]. The bottom color bar is the log of the shear stress in MPa. This solution is for shear stress in a half-space with a uniform viscosity of 10^{19} Pa s. Stress increases toward the sides and top, suggesting the gradients in the velocity and thus effectiveness of vug waves as a melt transport mechanism. Vug waves are predicted to migrate on the plane of maximum shear stress that has the strongest shear-stress gradient and are predicted to migrate toward the direction of increasing shear stress; for this analytical solution the direction of predicted vug wave migration is always straight toward the ridge axis. For spatially variable viscosities, such as those caused by temperature and pressure variations, and the extraction of water, Fe, and melt (i.e., the formation of a compositional lithosphere with $\eta_{cl} = 10^{21}$ Pa s), the resulting shear stresses will scale as the ratio of the shear viscosities.

and top of the melting region, suggesting that vug wave propagation up these axially converging shear planes could naturally focus melts toward the spreading axis.

4.2.2. Orogenic Vug Wave Applications

[44] Vug wave processes may also play an important role in orogenesis, with both magmatic and hydrous vug fluids acting to lubricate large shear and thrust faults, providing the physical mechanism underlying the "caterpillar-slip" deformation process imagined by *Oldham* [1921] and *Price* [1988]. Geologists have often noted the association of "frozen" magmatic intrusions with shear zones; such intrusions are found within both continental (e.g., Canadian Cordillera [*Hollister and Crawford*, 1986] and Alpine Ivrea Zone [*Handy and Streit*, 1999]) and oceanic (e.g., Lizard Ophiolite [*Allerton and MacLeod*, 1998] and Lanzo peridotite massif [*Boudier*, 1978; *Nicolas*, 1989]) settings. Perhaps the magmas are not only intruding into weaker shearing regions, but are also serving to weaken these shear zones by vug wave motion? In a mechanically similar vein, could the passage of hydrous vug waves created by dehydration reactions be an important weakening agent needed for nappe tectonics and the large-scale overthrusting found at convergent margins?

5. Conclusions

[45] While the analysis presented here is very simplistic, there are many potential applications of the variations we propose. These possibilities warrant further exploration in both theory (extensions to viscoelastic and viscous compaction variants) and observation (field and experimental). If vug waves are important in nature, then we must ask under what conditions do they nucleate, propagate, transform into other mechanisms, or freeze? Future tasks will be to study their behavior in controlled laboratory environments, and to search for observational techniques to image vug waves in the field.

Appendix A: Melt Overpressure Buildup During Pressure-Release Melting

[46] At the typical depths of plume and ridge melting, melting involves a net decrease in the density of the rock. Until the melt leaves the melting region, this will result in an overpressure. This effect is easy to evaluate in the limit where no melt escapes, and, as we will show, large overpressures are possible if melt escape is not exceedingly rapid. In the following approximation, we assume that as a rock parcel moves upward and melts, the rock + melt volume wants to increase but cannot. The pressure that must be exerted to compress the parcel to its original unmelted volume is what we call the "elastic self-pressure," P_{el}. We assume that for small melt fractions that are completely immobile, the volumetric strain will be elastic, and the stress will not relax by viscous creep on the timescale

that the melting occurs. This elastic self-pressure is defined as

$$P_{melt} = P_{lith} + P_{el}. \tag{A1}$$

[47] For simplicity, we will assume that the melting mantle has a uniform density of 3.3 $\frac{Mg}{m^3}$, and each increment of melt a density of 3.0 $\frac{Mg}{m^3}$, i.e., a density change of 10% during melting. Until melt escapes, the density reduction caused by the transformation from solid to melt must be accommodated by increased compression of the (viscoelastic) solid, which is the origin of the melting-induced overpressure. The elastic self-pressure, P_{el}, is compressive (<0) and is given by

$$P_{el} = -K\Delta, \tag{A2}$$

where K is the elastic bulk modulus of the rising mantle ($K \approx 100$ GPa) and Δ is the fractional volume change associated with melting,

$$\Delta = \frac{\Delta V}{V} = -\frac{\Delta \rho}{\rho} = \frac{\rho_{mantle} - \rho_{melt}}{\rho_{mantle}} \delta\phi, \tag{A3}$$

where $\delta\phi$ is the fractional volume of melt produced. $\delta\phi = (dF/dP)\delta P_{melt}$, where δP_{melt} is the change in the pressure of the melt, and the adiabatic melt productivity per unit of pressure release is $\frac{dF}{dP} = \frac{0.18}{GPa}$ (cf. *Phipps Morgan* [2001] for further discussion of the thermodynamics of pressure release melting]. (Note also that this P_{el} is the opposite of the effective pressure, $P_{eff} = P_{lith} - P_{melt}$ for low melt fractions, using the definitions in *Connolly and Podladchikov*, 1998.) Combining equations (A2) and (A3) with the relation above between $\delta\phi$ and δP_{melt} yields

$$P_{el} = -K\left(\frac{\rho_{mantle} - \rho_{melt}}{\rho_{mantle}}\right)(dF/dP)(\delta P_{melt}). \tag{A4}$$

($\Delta P_{el} \approx P_{el}$ when the initial state has $\phi = 0$.) From equation (21), the melt pressure change is the sum of the change in lithostatic pressure plus the elastic self-pressure induced by the density decrease associated with melting. Therefore, rewriting equation (21) as $\delta P_{melt} = \Delta P_{lith} + \Delta P_{el}$, and combining it with equation (A4), we get

$$\begin{aligned}\Delta P_{lith} &= \delta P_{melt} - \Delta P_{el} \\ &= \delta P_{melt}(1 - \Delta P_{el}/\delta P_{melt}) \approx 2.7\delta P_{melt}.\end{aligned} \tag{A5}$$

[48] In words, equation (A5) states that the change in pressure in an elastic solid melting by pressure release will only be about 1/2.7 or ≈40% of the external (lithostatic) pressure release, since the volume expansion induced by melting generates an internal elastic overpressure that accommodates 60% of the external pressure drop. For parameters appropriate to mid-ocean ridge melting, this internal overpressure is equal to 60% of the lithostatic pressure release. In other words, 50 m of ascent with melting but no melt escape will generate an internal overpressure of 1 MPa.

[49] Other implications of this simple analysis are that melt escape will lead to additional pressure release that generates an additional 1.5 times as much melt as the melt increment produced prior to escape, and that very small melt buildups, prior to any melt escape, generate large internal overpressures. For example, 50 m of lithostatic pressure release induces a (trapped) melt fraction buildup of only 10^{-4} that is associated with this internal pressure buildup of 1 MPa. Viscous relaxation will tend to relieve this overpressure. However, the appropriate viscosity for the creep relaxation of this partially molten material is its bulk viscosity, proportional to the shear viscosity of the rock divided by the melt fraction. Note that, without melt flow, the volumetric strain could not be anything but elastic because while the melt and solid are both elastically compressible, neither has an intrinsic bulk viscosity. For small melt fractions the appropriate viscoelastic relaxation time would be considerably longer than the 500–3000 years needed for the rock to ascend 50 m at the typical speeds associated with slow passive ridge upwelling (active upwelling would be associated with faster ascent than this). Clearly, this simple analysis suggests that even almost perfect melt escape can still be associated with significant (∼MPa) overpressure buildup within an ascending, melting region.

Acknowledgment

[50] We would like to thank Greg Hirth, two anonymous reviewers, and the editor, Peter van Keken, for helpful suggestions for improving the manuscript.

References

Aharonov, E., J. A. Whitehead, P. B. Kelemen, and M. Spiegelman (1995), Channeling instability of upwelling melt in the mantle, *J. Geophys. Res.*, *100*, 20,433–20,450.

Allerton, S., and C. J. Macleod (1998), Fault-controlled magma transport through the mantle lithosphere at slow-spreading ridges, in *Modern Ocean Floor Processes and the Geological Record*, edited by R. A. Mills and K. Harrison, *Geol. Soc. Spec. Publ.*, *148*, 29–42.

Atkinson, B. K., and P. G. Meredith (1987), Experimental fracture mechanics data for rocks and minerals, in *Fracture Mechanics of Rock*, edited by B. K. Atkinson, pp. 477–525, Elsevier, New York.

Boudier, F. (1978), Structure and petrology of the Lanzo peridotite massid (Piedmont Alps), *Geol. Soc. Am. Bull.*, *89*, 1574–1591.

Braun, M. G., and P. B. Kelemen (2002), Dunite distribution in the Oman Ophiolite: Implications for melt flux through porous dunite conduits, *Geochem. Geophys. Geosyst.*, *3*(11), 8603, doi:10.1029/2001GC000289.

Broek, D. (1987), *Elementary Engineering Fracture Mechanics*, Martinus Nijhoff, Zoetermeer, Netherlands.

Brune, J. N., P. A. Johnson, and C. Slater (1989), Constitutive relations for foam rubber stick-slip, *Seismol. Res. Lett.*, *60*, 26.

Brune, J., S. Brown, and P. A. Johnson (1993), Rupture mechanism and interface separation in foam rubber models of earthquakes: A possible solution to the heat flow paradox and the paradox of large overthrusts?, *Tectonophysics*, *219*, 59–67.

Connolly, J. A. D., and Y. Y. Podladchikov (1998), Compaction-driven fluid flow in viscoelastic rock, *Geodin. Acta*, *11*, 55–84.

Dahm, T. (2000), Numerical solutions of the propagation path and arrest of fluid-filled fractures in the Earth, *Geophys. J. Int.*, *141*, 623–638.

Daines, M. J., and D. L. Kohlstedt (1997), Influence of deformation on melt topology in peridotites, *J. Geophys. Res.*, *102*, 10,257–10,271.

Dragert, H., K. Wang, and T. S. James (2001), A silent slip event on the deeper Cascadia subduction interface, *Science*, *292*, 1525–1528.

Dragert, H., G. Rogers, and K. Wang (2004), Geodetic and seismic signatures of episodic tremor and slip beneath Vancouver island, British Columbia, *Eos Trans. AGU.*, Jt. Assem. Suppl., *85*(17), Abstract G23A-01.

Gerde, E., and M. Marder (2001), Friction and fracture, *Nature*, *413*, 285–288.

Goldstein, S. J., M. T. Murrell, D. R. Janecky, J. R. Delaney, and D. A. Clague (1991), Geochronology and petrogenesis of MORB from the Juan de Fuca and Gorda Ridges by ^{238}U-^{234}Th disequilibrium, *Earth Planet. Sci. Lett.*, *107*, 25–41.

Handy, M. R., and J. E. Streit (1999), Mechanics and mechanisms of magmatic underplating: Inferences from mafic veins in deep crustal mylonite, *Earth Planet. Sci. Lett.*, *165*, 271–286.

Heaton, T. H. (1990), Evidence for and implications of self-healing pulses of slip in earthquake rupture, *Phys. Earth Planet. Inter.*, *64*, 1–20.

Heimpel, M., and P. Olson (1994), Buoyancy-driven fracture and magma transport through the lithosphere: Models and experiments, in *Magmatic Systems*, edited by M. R. Ryan, pp. 223–240, Elsevier, New York.

Hirth, G., and D. Kohlstedt (2004), Rheology of the upper mantle and the mantle wedge: A view from the experimentalists, in *Inside the Subduction Factory*, *Geophys. Monogr. Ser.*, vol. 138, edited by J. Eiler, pp. 83–105, AGU, Washington, D. C.

Hollister, L. S., and M. L. Crawford (1986), Melt-enhanced deformation: A major tectonic process, *Geology*, *14*, 558–561.

Holtzman, B. K., N. J. Groebner, M. E. Zimmerman, S. B. Ginsberg, and D. L. Kohlstedt (2003), Stress-driven melt segregation in partially molten rocks, *Geochem. Geophys. Geosyst.*, *4*(5), 8607, doi:10.1029/2001GC000258.

Kelemen, P. B., G. Hirth, N. Shimizu, M. Spiegelman, and H. J. B. Dick (1997), A review of melt migration processes in the adiabatically upwelling mantle beneath oceanic spreading ridges, *Philos. Trans. R. Soc. London, Ser. A*, *355*, 283–318.

Lawn, B. (1993), *Fracture of Brittle Solids*, Cambridge Univ. Press, New York.

Lobkovsky, A., and J. S. Langer (1998), Dynamic ductile to brittle transition in a one-dimensional model of viscoplasticity, *Phys. Rev. E*, *58*(2), 1568–1576.

Lowry, A. R., K. M. Larson, V. Kostoglodov, and R. Bilham (2001), Transient fault slip in Guerrero, southern Mexico, *Geophys. Res. Lett.*, *28*(19), 3753–3756.

Lundstrom, C. C., D. E. Sampson, M. R. Perfit, J. Gill, and Q. Williams (1999), Insights into mid-ocean ridge basalt petrogenesis: U series disequilibrium from the Siquerios Transform, Lamont seamounts, and East Pacific Rise, *J. Geophys. Res.*, *104*, 13,035–13,048.

Macdonald, K. C. (1982), Mid-ocean ridges: Fine scale tectonic, volcanic, and hydrothermal processes within the plate boundary zone, *Annu. Rev. Earth Planet. Sci.*, *10*, 155–190.

Nicolas, A. (1989), *Structures of Ophiolites and Dynamics of Oceanic Lithosphere*, 380 pp., Springer, New York.

Oldham, R. D. (1921), Know your faults, *Geol. Soc. London Q. J.*, *77*, 77–92.

Ozawa, S., M. Murakami, and T. Tada (2001), Time-dependent inversion study of the slow thrust event in the Nankai trough subduction zone, southwestern Japan, *J. Geophys. Res.*, *106*, 787–802.

Pegoretti, A., and T. Ricco (2001), Creep crack growth in a short glass fibres reinforced polypropylene composite, *J. Mater. Sci.*, *36*, 4637–4641.

Phipps Morgan, J. (1987), Melt migration beneath mid-ocean spreading centers, *Geophys. Res. Lett.*, *14*, 1238–1241.

Phipps Morgan, J. (2001), Thermodynamics of pressure release melting of a veined plum pudding mantle, *Geochem. Geophys. Geosyst.*, *2*(4), doi:10.1029/2000GC000049.

Price, R. A. (1988), The mechanical paradox of large overthrusts, *Geol. Soc. Am. Bull.*, *100*, 1898–1908.

Renner, J., B. Evans, and G. Hirth (2000), On the rheologically critical melt percentage, *Earth Planet. Sci. Lett.*, *181*, 585–594.

Riley, G. N., Jr., and D. L. Kohlstedt (1991), Kinetics of melt migration in upper mantle-type rocks, *Earth Planet. Sci. Lett.*, *105*, 500–521.

Rubin, A. M. (1998), Dike ascent in partially molten rock, *J. Geophys. Res.*, *103*(B9), 20,901–20,919.

Shallamach, A. (1971), How does rubber slide?, *Wear*, *17*, 301–312.

Sims, K. W. W., et al. (2003), Aberrant youth: Chemical and isotopic constraints on the origin of off-axis lavas from the East Pacific Rise, 9°–10°N, *Geochem. Geophys. Geosyst.*, *4*(10), 8621, doi:10.1029/2002GC000443.

Sleep, N. H. (1984), Tapping of magmas from ubiquitous mantle heterogeneities: An alternative to mantle plumes?, *J. Geophys. Res.*, *89*(B12), 10,029–10,042.

Sobolev, A. V., and N. Shimizu (1993), Ultra-depleted primary melt included in an olivine from the Mid-Atlantic Ridge, *Nature*, *363*, 151–154.

Sobolev, A. V., and N. Shimizu (1994), The origin of typical N-MORB: The evidence from a melt inclusion study, *Min. Mag.*, *A58*, 862–863.

Spence, D. A., and D. L. Turcotte (1990), Buoyancy-driven magma fracture: A mechanism for ascent through the lithosphere and the emplacement of diamonds, *J. Geophys. Res.*, *95*(B4), 5133–5139.

Spiegelman, M., and D. McKenzie (1987), Simple 2-D models for melt extraction at mid-ocean ridges and island arcs, *Earth Planet. Sci. Lett.*, *83*, 368–377.

Stevenson, D. J. (1983), Magmatic transport by the migration of fluid-filled cracks, *Eos Trans. AGU*, *64*, 848.

Stevenson, D. J. (1986), On the role of surface tension in the migration of melts and fluids, *Geophys. Res. Lett.*, *13*(11), 1149–1152.

Stevenson, D. J. (1989), Spontaneous small-scale melt segregation in partial melts undergoing deformation, *Geophys. Res. Lett.*, *16*(9), 1067–1070.

Tada, H., P. C. Paris, and G. R. Irwin (1973), *The Stress Analysis of Cracks Handbook*, Del Res. Corp., Hellertown, Penn.

Takada, A. (1990), Experimental study on propagation of liquid-filled crack in gelatin: Shape and velocity in hydrostatic stress conditions, *J. Geophys. Res.*, *95*, 8471–8481.

Tolstoi, D. M. (1967), Significant of the normal degree of freedom and natural normal vibrations in contact friction, *Wear*, *10*, 199–213.

Turcotte, D., and G. Schubert (1982), *Geodynamics*, John Wiley, Hoboken, N. J.

Weertman, J. (1971), Theory of water-filled crevasses in glaciers applied to vertical magma transport beneath oceanic ridges, *J. Geophys. Res.*, *76*(5), 1171–1183.